On the Variability and Correlation of Surface Ozone and Carbon Monoxide Observed in Hong Kong Using Trajectory and Regression Analyses

WANG Tijian*[1,2] (王体健), K. S. LAM[2], C. W. TSANG[2], and S. C. KOT[3]

[1] *Department of Atmospheric Sciences, Nanjing University, Nanjing* 210093

[2] *Environmental Engineering Unit, Department of Civil & Structural Engineering, The Hong Kong Polytechnic University, Hong Kong*

[3] *Department of Mechanical Engineering, Hong Kong University of Science & Technology, Hong Kong*

(Received 17 December 2002; revised 15 June 2003)

ABSTRACT

This paper investigates, the variability and correlation of surface ozone (O_3) and carbon monoxide (CO) observed at Cape D'Aguilar in Hong Kong from 1 January 1994 to 31 December 1995. Statistical analysis shows that the average O_3 and CO mixing ratios during the two years are 32±17 ppbv and 305±191 ppbv, respectively. The O_3/CO ratio ranges from 0.05 to 0.6 ppbv/ppbv with its frequency peaking at 0.15. The raw dataset is divided into six groups using backward trajectory and cluster analyses. For data assigned to the same trajectory type, three groups are further sorted out based on CO and NO_x mixing ratios. The correlation coefficients and slopes of O_3/CO for the 18 groups are calculated using linear regression analysis. Finally, five kinds of air masses with different chemical features are identified: continental background (CB), marine background (MB), regional polluted continental (RPC), perturbed marine (P*M), and local polluted (LP) air masses. Further studies indicate that O_3 and CO in the continental and marine background air masses (CB and MB) are positively correlated for the reason that they are well mixed over the long range transport before arriving at the site. The negative correlation between O_3 and CO in air mass LP is believed to be associated with heavy anthropogenic influence, which results from the enhancement by local sources as indicated by high CO and NO_x and depletion of O_3 when mixed with fresh emissions. The positive correlation in the perturbed marine air mass P*M favors the low photochemical production of O_3. The negative correlation found in the regional polluted continental air mass RPC is different from the observations at Oki Island in Japan due to the more complex O_3 chemistry at Cape D'Aguilar.

Key words: ozone, carbon monoxide, trajectory

1. Introduction

O_3 and CO are two important trace gases in the troposphere. As we know, O_3 is a critical oxidant in the troposphere, which plays a key role in biogeochemical cycles and global climate change. O_3 is considered to be an important greenhouse gas because of its absorption of terrestrial longwave radiation. Surface O_3 in sufficiently high concentrations can do harm to human health and vegetation (Parrish, 1998). As to CO, it provides a relatively long-lived tracer of anthropogenic emissions, which helps to differentiate O_3 sources. In a relatively clean atmosphere, CO acts as a precursor of O_3. On the other hand, about 70% of OH reacts with CO (Wayne, 1991), causing CO to be a major sink of OH. A secular increase in CO can have a feedback effect on OH abundance (Khalil and Rasmussen, 1988). Furthermore, O_3 and CO can be easily and accurately measured by instrumentation which can be operated long-term in unattended locations. For the above reasons, O_3 and CO have become the two species of particular interest to scientists.

Surface O_3 and CO have been measured at Cape D'Aguilar, Hong Kong since November 1993 as a com-

*E-mail: tjwang@nju.edu.cn

ponent of APARE (East Asia-North Pacific Regional Experiment). Wang et al. (1997) analyzed the trace gases measured during the PEM-WEST B campaign in winter-spring 1994. They found that the site was often under the impact of fresh continental emissions (including urban Hong Kong) during the periods of continental outflow. The intermittent ozone-pollution episodes observed at the site were reported by Wang et al. (1998). Chan et al. (1996, 1998a) reported the highest O_3 concentration at the surface and below 2 km in late-fall and early-winter. The 1994 seasonal, temporal, and spatial variation of the surface O_3 at Hong Kong was analyzed by Chan et al. (1998b). Based on different surface pressure patterns in Asia, the seasonal variation of surface O_3 has been found to be governed by the Asia Monsoon. Liu et al. (1999) investigated the springtime high ozone events in the lower troposphere from Southeast Asian biomass burning.

There are few previous studies of the correlation of O_3 and CO at the Hong Kong monitoring site. Lam et al. (1996) found that surface O_3 and CO were positively correlated in summer and negatively correlated in winter based on 1994 data. The relationship between O_3 and CO at other sites in the world have been investigated by many scientists. For example, Parrish et al. (1993) reported a positive correlation in marine air mass. Derwent et al. (1994) observed a negative correlation between O_3 and CO within a polluted air mass during the winter season. As discussed by Parrish et al. (1998), the O_3 and CO relationship can delineate the seasons and regions in which photochemical production of O_3 from anthropogenic precursors dominates photochemical sinks. Pochanart et al. (1999) pointed out that correlation between O_3 and CO can be used to demonstrate photochemical activities on a regional scale. These studies have shown the great importance of the relationship between surface O_3 and CO as an indicator of anthropogenic air pollution.

As described elsewhere, in the troposphere during the daytime, NO_2 can be photolysed to form an oxygen atom that can then combine with oxygen to form O_3. The reactions are as follows:

$$NO_2 + h\nu \rightarrow NO + O\,, \tag{1}$$

$$O + O_2 \rightarrow O_3\,. \tag{2}$$

Reactions (1) and (2) can be revised by the rapid reaction of NO with O_3.

$$NO + O_3 \rightarrow NO_2 + O_2\,. \tag{3}$$

The oxidation of CO in the boundary layer also generates O_3. CO can be oxidized in a chain reaction. Following an initial attack by OH, a hydrogen atom is formed which combines with oxygen to form HO_2, which can transform NO to NO_2.

$$CO + OH \rightarrow CO_2 + H\,, \tag{4}$$

$$H + O_2 \rightarrow HO_2, \tag{5}$$

$$HO_2 + NO \rightarrow OH + NO_2\,. \tag{6}$$

In remote locations, which are largely free from anthropogenic emissions and with low concentrations of NO_x and CO, little O_3 is formed.

This paper focuses on the variation and correlation of surface O_3 and CO observed at Cape D'Aguilar. Hourly O_3 and CO mixing ratios as well as the O_3/CO ratio are discussed. In order to understand the chemical features of different air masses coming to the monitoring site, the O_3 and CO data are categorized into six groups based on the trajectory and cluster analyses. In each group, three subgroups are further sorted out according to CO and NO_x mixing ratios. The relationship between surface O_3 and CO is investigated by use of linear regression analysis. Finally, the chemical features of air masses represented by each group are identified.

2. Methodology

2.1 *Monitoring site*

The monitoring station was established in 1993 by the Hong Kong Polytechnic University in order to measure the composition of the atmosphere and to study the processes affecting the chemistry and transport of air pollution in East Asia. It is located at Cape D'Aguilar (22.2°N, 114.3°E, 60 m above sea level) on the southeast tip of Hong Kong Island and was built on the top of a cliff facing the South China Sea (Fig. 1). The station is about 20 km away from the city center.

Because of its location on the coast between the Asian continent and the South China Sea, under the strong influence of the Asia monsoon, the site can receive continental air masses in winter and marine air masses in summer. During Northern Hemisphere winter, an intense high pressure belt develops in the northern part of the Asian continent causing a general outflow pattern on the surface. In Northern Hemisphere summer, the situation is reversed. Southwest to southeast monsoon winds cause large scale inland flow of the marine air mass along the coast of the Asian continent. Air masses from the continent and ocean will experience different long-range transport of trace gases to this station. In spring, the winter monsoon weakens. However, the continent is still cold. Occasional infiltration of marine air along the coast brings wet and foggy weather. Humidity is high at this time of the

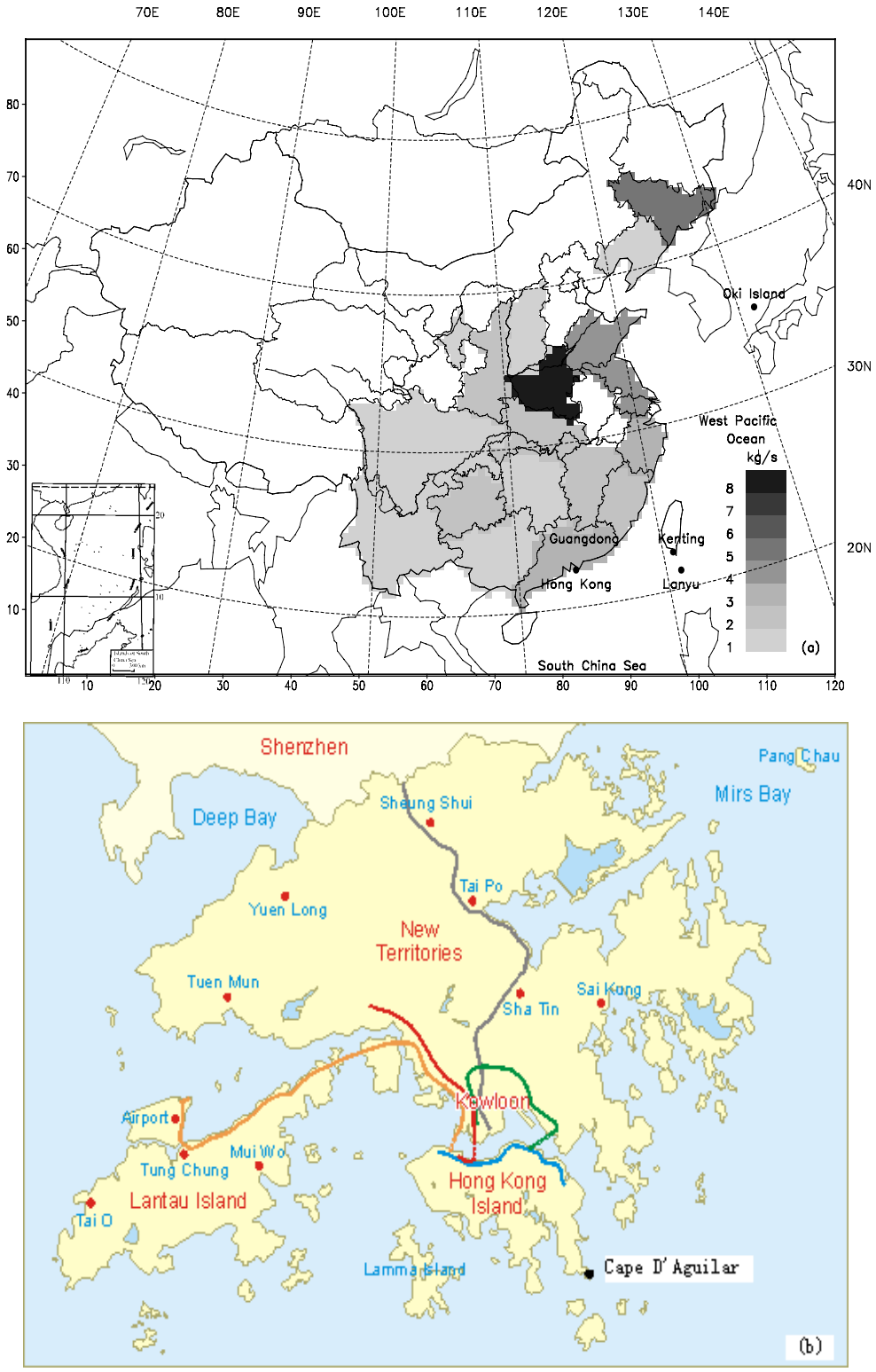

Fig. 1. (a) Location of Hong Kong and anthropogenic CO emission strength over China (kg s^{-1}); (b) Location of Cape D'Aguilar.

year. In fall, the climate is described as weak continental. With the retreating summer monsoon, the weather is generally warm, dry, and pleasant. Generally, the climate of the site is humid subtropical. It has four seasons characterized by a marked change of wind direction, temperature, humidity, and rainfall. The prevailing surface wind direction measured at the station is easterly. The site has a view of the sea greater than 180 degrees from the northeast to the southwest. Over 60% of the time, the local wind is from the sea and the station is upwind of Victoria Harbor.

2.2 *Measurement*

Surface O_3, CO, and NO_x have been collected at Cape D'Aguilar since December 1993. O_3 is measured with a commercial UV photometric analyzer (Thermo Environment Instruments Inc., Franklin, MA, Model 49). The detection limit and precision of the instrument are both 2 ppbv (signal to noise ratio 2:1 at the $\pm 2\sigma$ noise level, with 2 min. averaging time). Its sensitivity change is less than 2% over one year of observation.

CO measurement is obtained with a gas filter correlation, nondispersive infrared absorption instrument (Thermo Environmental Instruments Inc., Model 48). The precision of the instrument for 1 hour average is estimated to be 3.4% at the 650-ppbv level. The instrument is determined to be linear to within 3% from 100 to 2000 ppbv and has a 10-s signal averaging period and about 1.1 L min^{-1} sample flow rate.

NO_x measurement is made using a commercial chemiluminescence low level NO_x analyzer (Thermo Environmental Instruments Inc., Model 42S). The equipment automatically switches between NO-NO_x-zero mode. The prereactor mixes the ambient sample with ozone prior to the reaction chamber giving a dynamic zero reading. Once every 4 hours, the analyzer switches into a 3-step calibration sequence. Artifact checks are performed for 5 minutes by injecting Purafil-scrubbed zero air. NO sensitivity is then checked for 6 minutes using a standard addition technique. An NO_2 sensitivity check follows for 6 minutes using standard gas generated from a permeation tube.

The data logger computes a 1-min average for each of the quantities measured. The raw data files are then decoded and separated into individual time series. The three time series are then hourly averaged. All subsequent data analysis in this paper is based on the hourly averaged data.

2.3 *Backward trajectories*

Isentropic backward trajectories are used to indicate the air mass transport path under the assumption of an adiabatic displacement of the air parcels. The reason for choosing isentropic backward trajectories is that they are usually considered to reflect more realistically the vertical motion of an adiabatic atmosphere (Harris et al., 1990). The given trajectory produced by the model should be reasonably representative of the large scale circulation and can be used to suggest potential source regions. Although the trajectory method has been a popular tool to trace air mass transport, uncertainty due to convection, evaporation, and condensation (diabatic processes) are associated more with isentropic trajectory models. As discussed by Harris et al. (1992), all trajectory models are subject to uncertainty arising from interpolation of sparse meteorological data, assumptions regarding vertical transport, observational errors, subgrid-scale phenomenon, turbulence, convection, evaporation, and condensation.

Backward trajectories from Hong Kong during the years 1994 to 1995 are computed by the NOAA-HYSPLIT4 model (Draxler et al., 1997, 1998). Input to the trajectory model is in the form of 1.125 degree latitude-longitude gridded meteorological parameters and topography furnished by the European Centre for Medium range Weather Forecast (ECMWF). Five-day backward trajectories arriving at 1000 m above sea level are calculated four times every day, at 0000, 0600, 1200 and 1800 UTC, with a time step of one hour. Since the study region has a complex terrain, the height of the mixing layer is relatively high, thus 1000 m is chosen for trajectory calculations to diminish the effects of surface friction and to represent winds in the boundary layer.

2.4 *Cluster analysis*

The two years of trajectories are clustered into six groups. Trajectory clustering takes a collection of trajectories and identifies several unique clusters, or subsets, of the collection. Initially, each trajectory is defined to be a cluster with zero spatial variance, where the cluster spatial variance is the sum of the squared distances between the cluster's component trajectories and their mean. Successive steps combine two clusters that result in the minimum total spatial variance (TSV), where TSV is the sum of all the cluster spatial variances. In the first several steps the TSV increases greatly, then for much of the clustering it typically increases at a small, generally constant rate, but at some point it again increases rapidly, indicating that the clusters being combined are not very similar. The step just before this large increase in TSV gives the final number of clusters, which is found to be six for our trajectory collection (Stunder, 1996).

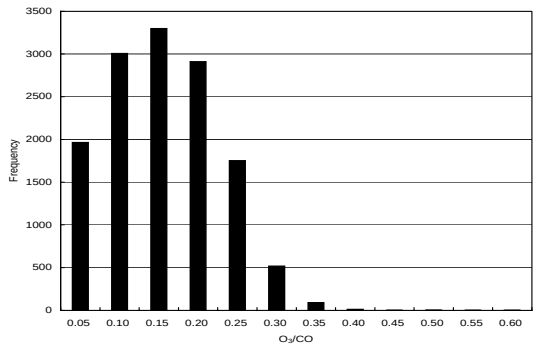

Fig. 2. Frequency distribution of O_3/CO ratio in 1994–1995.

3. Results and discussions

3.1 *Measurements*

3.1.1 O_3, CO, *and* NO_x *mixing ratios*

The statistics of the observed hourly surface O_3, CO, and NO_x mixing ratios in the two years are listed in Table 1. The CO mixing ratio has a broad range from 44 to 1280 ppbv, whereas the O_3 and NO_x mixing ratios are from 1 to 162 ppbv and from 0.2 to 143 ppbv, respectively. Most of the O_3, CO, and NO_x mixing ratios are within the ranges of CO<1000 ppbv, O_3 <80 ppbv, and NO_x <10 ppbv. Episodes with extremely high O_3 can be found occasionally. High CO (>1000 ppbv) cases are always accompanied by low O_3 (<20 ppbv). When the O_3 mixing ratio is greater than 80 ppbv, CO usually ranges from 300 to 1000 ppbv. The two year average of the O_3, CO, and NO_x mixing ratios are 32±17 ppbv, 305±191 ppbv, and 7±9 ppbv, respectively. Apparently, the observed O_3, CO, and NO_x show the characteristics of all types of clean air masses as well as polluted air masses on regional or local scales. It is necessary that the entire dataset be classified in order to understand the transport and chemical features of different air masses arriving at the monitoring station.

3.1.2 O_3 *to* CO *ratio*

It was reported that the O_3 to CO ratio can give an estimate of amount of O_3 exported to the troposphere over the ocean from regions of anthropogenic activity (Parrish et al., 1993). Therefore, hourly O_3/CO ratios are calculated with their frequency distribution illustrated in Fig. 2. It shows that O_3/CO ratios are between 0.05 and 0.6 ppbv/ppbv. The mode of O_3/CO is 0.15. The cases with $0.1<O_3/CO<0.2$ account for 69% of the total dataset.

The significant variations of O_3/CO imply that air masses with different chemical features were observed at the site. Overall, the low O_3/CO cases indicated that the local influence may be important in which CO and NO_x are always high and O_3 is titrated resulting in a low mixing ratio. The high O_3/CO cases suggest that the air masses probably originated from relatively clean regions with low CO, or O_3 was photochemically built up when the air masses passed over the emission areas during their travel to the site. It is believed all cases have signatures governed by complex transport and chemical processes which will be described in section 3.2.

3.2 *Air mass classification*

3.2.1 *General classification*

In order to identify the different air masses arriving at the site, isentropic backward trajectories are calculated for the period 1994–1995. The trajectories are then clustered into six groups which are illustrated in Fig. 3. Two groups (C-E and C-N) originate from Europe and Northern China. They are named as "continental" trajectories since they traveled south across China before reaching the site. The other three groups (M-SW, M-SE, and M-E) originate from the oceans, arriving at the site from the southwest, southeast, and east, respectively. They are called "marine" trajectories because they spent most of their time traveling over the sea. The last group (L) has no defined path and the trajectories meandered close to Hong Kong with very low wind speed. They are referred to as "loop" trajectories.

3.2.2 *Sub-classification*

In fact, when we check the data assigned to the

Table 1. Statistics of observed O_3, CO, and NO_x during 1994–1995 (ppbv).

	O_3	CO	NO_x
Average	32	305	7
Standard deviation	17	191	9
Root mean square	36	360	11
Average deviation	14	154	4
Minimum	1	44	0.2
Maximum	162	1280	143

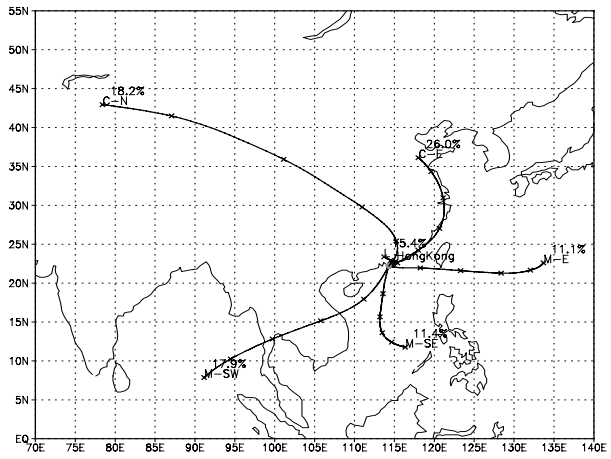

Fig. 3. Cluster analysis of backward trajectories during 1994–1995.

same type of trajectory, the O_3 and CO mixing ratios still show significant differences, implying that there are various chemical features in air masses having the same trajectory. Since NO_x can be used to identify fresh emissions due to its short residence time, and since CO has been considered to be an inert trace gas as well as a good indicator of anthropogenic emission, three concentration sets are further sorted out in each trajectory group with the criteria of (1) NO_x <5 ppbv and CO<150 ppbv, (2) NO_x >5 ppbv and CO>150 ppbv, (3) NO_x >5 ppbv. They are named as LNLC (Low NO_x and Low CO), LNHC (Low NO_x and High CO), and HNAC (High NO_x and All CO) groups, respectively. Such identification aims to classify the chemical features of air masses which belong to the same trajectory group. Finally, 18 groups are obtained. Table 2 gives the case number of each group. The averaged O_3 and CO mixing ratios are listed in Table 3 and Table 4, respectively. They will be discussed in sections 3.2.3, 3.2.4, and 3.2.5 in detail.

3.2.3 O_3 *and* CO *mixing ratios in continental air mass*

The O_3 and CO mixing ratios in the LNLC-C-E group are 34 ppbv and 139 ppbv, which are comparable to the continental background values from Pochanart et al. (1999). They found that CO in the clean continental background air mass was between 120 and 208 ppbv while O_3 was from 32 to 45 ppbv. The CO mixing ratio in the perturbed continental background air mass ranges from 142 to 236 ppbv and the counterpart for O_3 is between 35 and 51 ppbv.

The O_3 and CO mixing ratios are 43 and 325 ppbv in the LNHC-C-E group, while they are 48 and 360 ppbv in the LNHC-C-N group. Both O_3 and CO in these two groups have relatively higher mixing ratios (46 and 343 ppbv on average), reflecting a typical signature of the regional polluted air mass. Trajectory analysis indicates that the air mass of the C-E group originates from North China and passes over the East China coastal region, and that of the C-N group originates from Northwest China and then travels through Central China. In particular, the two groups of air masses cross over the Pearl River Delta region, the most developed industrial area in Guangdong Province, before arriving at the site. From Fig. 1a, anthropogenic emissions are strong in the East China coastal region, Central China, and Guangdong

Table 2. Hourly case numbers of each group.

	C-E	C-N	M-SW	M-SE	M-E	L
LNLC	46	–	1495	491	345	–
LNHC	2384	1119	337	81	585	757
HNAC	1343	1210	1054	551	651	1115

Table 3. Averaged O_3 mixing ratio of each group (ppbv).

	C-E	C-N	M-SW	M-SE	M-E	L
LNLC	34±10	–	16±6	15±6	20±8	–
LNHC	43±11	48±10	36±13	31±11	39±9	35±11
HNAC	33±15	43±16	15±11	13±11	25±21	30±15

Table 4. Averaged CO mixing ratio of each group (ppbv).

	C-E	C-N	M-SW	M-SE	M-E	L
LNLC	13±98	–	92±19	90±20	106±23	–
LNHC	325±141	360±117	222±60	183±35	254±86	467±149
HNAC	456±185	420±134	148±98	156±73	312±189	522±174

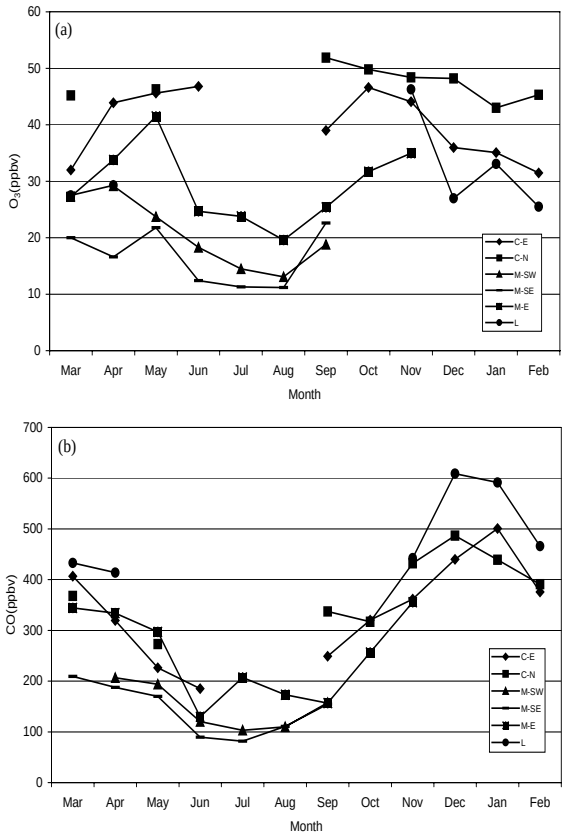

Fig. 4. Seasonal variations of (a) O_3, (b) CO mixing ratios in different air masses.

Province as indicated by high CO emission strength (Streets, 2000). Therefore, O_3 can be photochemically produced when the air masses pass through the regions with strong anthropogenic activity. Similar observations have been obtained at other sites in East Asia. For example, O_3 and CO concentrations in the continental outflow are about 44–57 ppbv and 180–271 ppbv at Oki Island in Japan (Pochanart et al., 1999). Although the 46 ppbv O_3 and 343 ppbv CO are representative of the signature of the regional polluted continental air mass, O_3 is lower and CO is higher at Cape D'Aguilar compared to Oki Island. The enhanced CO and depleted O_3 are believed to be caused by the complex photochemistry process when the air masses pass over Guangdong Province and capture abundant anthropogenic emission. This will be discussed further in section 3.3.

The CO mixing ratios in the HNAC-C-E and HNAC-C-N groups are 456 and 420 ppbv, which are about 131 and 60 ppbv higher than the LNHC-C-E and LNHC-C-N groups. The higher CO mixing ratios in the two groups suggest that the influence of fresh anthropogenic emissions becomes more important. Since the site is near to the urban area of Hong Kong, sometimes it can be affected by local emissions. The O_3 mixing ratios in the HNAC-C-E and HNAC-C-N groups are 33 and 43 ppbv. They are about 10 and 5 ppbv lower compared to the LNHC-C-E and LNHC-C-N groups. The relatively lower O_3 and higher CO in these two groups reveal the fact that O_3 can be depleted when it is mixed with the polluted air mass marked by higher CO and O_3 precursors.

The seasonal variations of the O_3 and CO mixing ratios in the entire C-E and C-N groups are described in Fig. 4. These two groups of air masses are encountered in winter, autumn, and spring. O_3 in C-E and C-N is 39 and 46 ppbv, respectively, while CO is 369 and 391 ppbv. The O_3/CO ratio in the continental air masses at Cape D'Aguilar is about 0.11, which is much lower than the values of 0.18 at Oki Island (Arimoto et al., 1997) and 0.2 at Lanyu (Liu et al., 1999), showing that the station is more influenced by anthropogenic emissions. The O_3 mixing ratio reaches its maximum in autumn. As discussed by Lam et al. (2001), the O_3 maximum in autumn is attributed to the long range transport of high O_3 precursors within the polluted continental air masses as well as the photochemical buildup in the dry and sunny weather conditions in the low latitude region.

3.2.4 O_3 *and* CO *mixing ratios in marine air mass*

The signatures of the LNLC-M-SW and LNLC-M-SE groups are very similar with an average of 16 ppbv O_3 and 91 ppbv CO. These two groups have the characteristics of a clean marine air mass. The observed O_3 within trajectories coming from the South China Sea to Okinawa and Kenting were 22±2 ppbv and 17±3 ppbv during PEM-WEST A (Akimoto et al., 1996). At the Lanyu monitoring site in Taiwan, the O_3 mixing ratio varied between 13 and 18 ppbv and the CO mixing ratio varied from 120 to 140 ppbv in the summer of 1995 (Liu et al., 1999). Furthermore, the typical trajectories indicate that the air masses of the two routes come from the South China Sea and seldom touch the land before arriving at the site. For the above two reasons, it is plausible to consider the values of 16 ppbv O_3 and 91 ppbv CO as the signature of the marine background of the South China Sea. The O_3 and CO mixing ratios in the LNLC-M-E group are 20 and 106 ppbv, which are close to the background of the West Pacific Ocean (15 ppbv O_3 and 100 ppbv CO) as reported by Akimoto et al. (1996). This fact suggests that the LNLC-M-E route is representative of the background marine air mass from the West Pacific.

Table 5a. Correlation coefficient between O_3 and CO in each group.

	C-E	C-N	M-SW	M-SE	M-E	L
LNLC	0.59	–	0.47	0.51	0.66	–
LNHC	–0.36	–0.31	0.32	0.30	0.23	–0.40
HNAC	–0.44	–0.33	0.31	0.31	0.21	–0.27

Table 5b. Slope of the O_3 and CO correlation in each group.

	C-E	C-N	M-SW	M-SE	M-E	L
LNLC	0.800	–	0.139	0.151	0.243	–
LNHC	–0.028	–0.026	0.069	0.091	0.114	–0.030
HNAC	–0.036	–0.039	0.035	0.045	0.023	–0.023

The LNHC-M-SW and LNHC-M-SE groups have an average O_3 value of 34 ppbv and CO value of 203 ppbv. The typical trajectories show that the air masses of the two groups pass through the South or Southeast Asian countries and touch the land 1–2 days before reaching the site, causing them to be occasionally perturbed. The relatively higher O_3 and CO in the LNHC-M-E group compared to the LNLC-M-E group indicate the possible influence of anthropogenic emissions from the industrial Taiwan Island or sea-going ships on the observed results at the site.

The O_3 and CO mixing ratios in the HNAC-M-E group are 25±21 ppbv and 312±189 ppbv. The typical trajectory comes from the east and has a marine signature. However, the air mass can be perturbed to a certain extent due to the possible emissions from Taiwan Island and nearby ships. Overall, the characteristics of the air mass in this group are very similar to those of LNHC-M-E.

Figure 4 also gives the annual trend of the O_3 and CO mixing ratios in the M-SW, M-SE, and M-E groups. It is obvious that the marine-originating air masses tend to appear in summer, spring, and autumn. They usually have low O_3 (15–29 ppbv) and CO (128–246 ppbv) mixing ratios compared to the continental air masses. The O_3/CO ratio in the marine air masses is about 0.12 which is very comparable with the value of 0.11 observed at Lanyu (Liu et al., 1999). The lowest O_3 and CO are found in July for the M-SW/M-SE groups and in June for the M-E group. O_3 and CO exhibit similar signatures in the M-SW and M-SE routes, both of which are lower than their counterparts in the M-E route.

3.2.5 O_3 *and* CO *mixing ratios in local influenced air mass*

For the LNHC-L and HNAC-L groups, the O_3 mixing ratios are 35 and 30 ppbv, while the CO mixing ratios are 467 and 522 ppbv. The signatures of the LNHC-L and HNAC-L groups are similar to the HNAC-C-E and HNAC-C-N groups except that the O_3 mixing ratio is lower. The high CO concentration implies anthropogenic emissions. Since the trajectories have no defined path and usually meander close to Hong Kong with low wind speed, the air masses are susceptible to contamination by local emissions which can result in O_3 titration. For this reason, the O_3 mixing ratio is not very high compared to the regional polluted air masses LNHC-C-E and LNHC-C-N. As shown in Fig. 5, the L groups can always be found in winter and spring with the highest CO mixing ratios in all six trajectory groups.

3.3 O_3 *and* CO *relationship in each group*

Since CO was found to be both a good indicator of anthropogenic pollutants with a relatively long residence time and one of the O_3 precursors, the correlation between O_3 and CO can be applied to demonstrate photochemical activities on a regional scale (Pochanart et al., 1999). To understand the surface O_3 and CO relationship observed at Cape D'Aguilar, a simple linear regression between hourly O_3 and CO mixing ratios is performed for each classified group. The correlation coefficients and slopes for the two year dataset are listed in Table 5.

In general, a significant negative correlation between O_3 and CO is observed in the continental air masses (C-E and C-N) and loop trajectories (L), while a positive correlation is found in air masses which have marine origination (M-SW, M-SE, and M-E). Because the correlation coefficients of the O_3 and CO relationship are not high for some groups, *t*-tests were carried out to determine the statistical significance of the correlation. The calculations show that the correlations between O_3 and CO are significant at the 95% confidence level for all groups.

In Table 5, the correlation coefficients between O_3 and CO in all the LNLC groups are positive with values between 0.47–0.66. Extremely low CO mixing ra-

tios in the LNLC groups highly suggest that the air masses are very clean, thus, there the lowest photochemical production of O_3 will occur. Since the air masses in the LNLC groups have been well mixed over the long range transport, it is not unexpected for O_3 and CO to be significantly positively correlated in these routes. On the other hand, the marine boundary layer in low latitudes is generally a region of low NO_x and high sunlight and water vapor, which can result in rapid photochemical loss of O_3 and CO (Parrish et al., 1998). The positive correlation between O_3 and CO in LNLC-M-SW, LNLC-M-SE, and LNLC-M-E can be attributed to the fact that they are believed to be simultaneously removed by photochemical processes in regions isolated from sources of nitrogen oxides.

O_3 and CO display negative correlation in the LNHC-C-E and LNHC-C-N groups which have continental origin. Both the of O_3 and CO mixing ratios in these two groups are higher compared to the LNLC-C-E group. The elevated CO implies anthropogenic influence. As a consequence, O_3 can be photochemically produced on a regional scale over the long range transport before reaching the site. Pochanart et al. (1999) reported a positive correlation between O_3 and

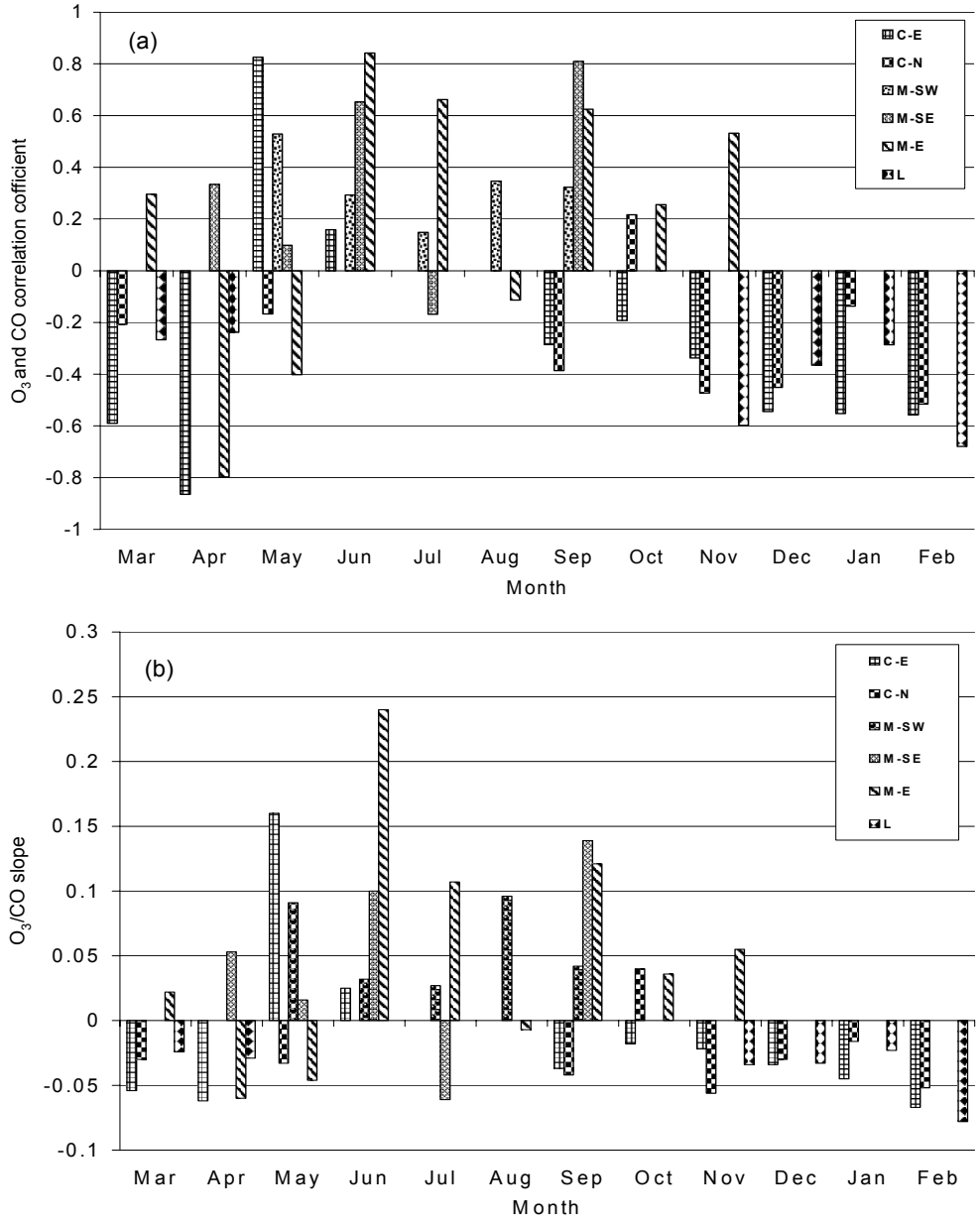

Fig. 5. (a) Seasonal variation of O_3 and CO correlation coefficient for each air mass; (b) Seasonal variation of $\Delta O_3/\Delta CO$ slope for each air mass.

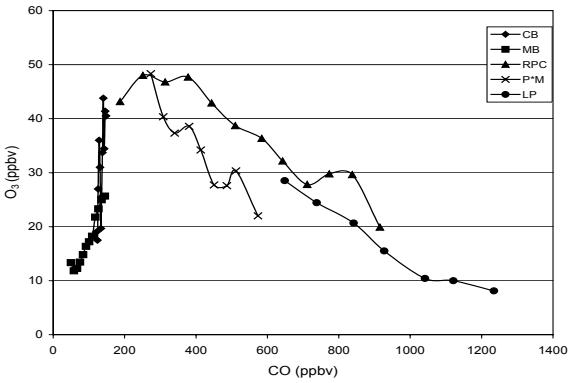

Fig. 6. Conditional average O_3 and CO relationship in each group.

CO in regionally polluted continental air mass arriving at Oki Island. However, things are different at Cape D'Aguilar. The possible cause for the negative correlation can be explained by the different O_3 chemistry along the air mass trajectories. As the air mass travels across South China, especially the Pearl River Delta region, it easily captures strong anthropogenic emissions and O_3 is produced photochemically when its precursors are regionally dispersed. In contrast, as the air masses pass over Hong Kong city, the abundance of precursors can result in O_3 loss through the titration process. The complex O_3 chemistry during the different periods of the transport process can explain the negative correlation between O_3 and CO. The relatively higher CO mixing ratios in the LNHC-M-SW, LNHC-M-SE, and LNHC-M-E groups suggest that the marine air masses were perturbed (a little polluted) with a small amount of O_3 precursors, therefore, O_3 was able to be photochemically produced, which led to the positive correlation observed in these groups.

A negative correlation was found in the HNAC-C-E and HNAC-C-N groups with correlation coefficients of –0.44 and –0.33, which implies that O_3 can be removed through chemical reactions related to the titration process. One possible factor may contribute to this negative correlation. That is, a mixing with fresh emissions of high NO_x often depletes O_3 in the near field. Under this condition, O_3 can be lost through the reactions with NO or NO_2 The reasons for the positive correlation in the HNAC-M-SW, HNAC-M-SE, and HNAC-M-E groups are similar to those for the LNHC-M-SW, LNHC-M-SE, and LNHC-M-E groups, which also reflect the O_3 production in the perturbed marine air mass.

The O_3 and CO are negatively correlated in air masses which have loop trajectories (LNHC-L and HNAC-L). A very high CO mixing ratio favors the strong local influence and the O_3 titration process can happen under this condition due to the over-abundance of precursors. A similar negative correlation was discussed by Wang et al. (1997), in which it was found that the titration of O_3 by local sources upwind of the station reduced the secondary pollutants to low levels.

In addition, distinct seasonal variations in the O_3 and CO relationship are found in each type of trajectory, which is illustrated in Fig. 5. It shows that in the continental air masses (C-E, C-N), the correlation coefficients between O_3 and CO are negative in winter with values from –0.56 to –0.2. This negative correlation is very strong in December and February for these two groups. The $\Delta O_3/\Delta CO$ slopes in the C-E and C-N groups range from –0.07 to –0.03. O_3 and the CO correlation coefficients in the marine air masses (M-SW, M-SE, and M-E) are usually positive in summer (0.2–0.8); the maximum is found to be 0.84 in the M-E air mass in June with $\Delta O_3/\Delta CO$ being 0.24.

3.4 *Identification of chemical features of air masses in each group*

In consideration of the classification results based on trajectories and variations of O_3 and CO levels as well as their relationship in each group, the chemical features of the different air masses approaching the site are identified and summarized in Table 6. Generally, five kinds of air masses were observed at Cape D'Aguilar, which have the following signatures: continental background (CB), marine background (MB), regional polluted continental (RPC), perturbed marine (P*M), and local polluted (LP) air masses. The conditional average O_3 and CO of the five groups are presented in Fig. 6. It clearly shows the distinctive O_3 and CO mixing ratios as well as their correlation, reflecting the different chemical features in each kind of air mass.

Table 6. Chemical features of air masses in each group.

	C-E	C-N	M-SW	M-SE	M-E	L
LNLC	CB	–	MB	MB	MB	–
LNHC	RPC	RPC	P*M	P*M	P*M	LP
HNAC	LP	LP	P*M	P*M	P*M	LP

C: Continental; M: Marine; B: Background; R: Regional; L: Local; P: Polluted; P*: Perturbed

4. Summary and conclusions

By use of trajectory and regression methods, we present a study on the variability and correlation of surface O_3 and CO observed at the coastal site Cape D'Aguilar of Hong Kong from January 1994 to December 1995. Statistical analysis shows that the average O_3 and CO mixing ratios during the two years are 32±17 ppbv and 305±191 ppbv. The O_3/CO ratio has a wide range from 0.05 to 0.6.

The raw data are categorized into 18 groups based on isentropic backward trajectories as well as CO and NO_x mixing ratios. The correlation coefficients and $\Delta O_3/\Delta CO$ slopes are then calculated using linear regression. Eventually, five kinds of air masses with different chemical features are identified, including continental background (CB), marine background (MB), regional polluted continental (RPC), perturbed marine (P*M), and local polluted (LP) air masses.

O_3 and CO in the continental background air masses have average concentrations of 34 ppbv and 139 ppbv. In contrast, the marine background air masses show 13–20 ppbv O_3 and 90–156 ppbv CO. Much higher O_3 (43–48 ppbv) and CO (325–360 ppbv) are observed in the regional polluted continental air masses. O_3 is 25–39 ppbv and CO is 183–312 ppbv in the perturbed marine air masses.

As for the O_3 and CO relationship, investigations show that there is a positive correlation between O_3 and CO in the continental and marine background air masses (CB and MB). The negative correlation in air masses with local influence (LP) is attributed to the enhancement of anthropogenic sources indicated by high CO and NO_x and depletion of O_3 when mixed with fresh emissions. A positive correlation is also found in the perturbed marine air masses (P*M), which favor a lower photochemical O_3 production. O_3 and CO display a negative correlation in the regional polluted continental air masses (RPC), which is very different from the signature of the air mass observed at Oki Island. The difference implies complex photochemical features at Cape D'Aguilar and raises the scientific value of new tracers, such as NO_x, NMHC, and aerosols, which need to be measured to further explain the data. Additionally, the analyses show the limitations of the trajectory method, which needs to be combined with other tracers to determine the chemical features of the different air masses.

The results obtained in this study establish the significance of long-term observations at the coastal site of Cape D'Aguilar in Hong Kong since the location of the site allows for monitoring of several kinds of air masses with different chemical features. In particular, Cape D'Aguilar can serve as an important baseline station to observe the long range transport of air pollutants with more complex photochemistry due to anthropogenic emissions from the Asian continent.

Acknowledgments. This work was supported by the Research Grant Council of Hong Kong (Grant No. POLYU 5047/98E). Sincere thanks are given to the two anonymous reviewers who gave useful suggestions for this paper.

REFERENCES

Akimoto, H., and coauthors, 1996: Long range transport of ozone in the East Asian Pacific Rim region. *J. Geophys. Res.*, **101**(D1), 1999–2010.

Arimoto, R., and coauthors, 1996: Relationships among aerosol constituents from Asia and the North Pacific during PEM-WEST A. *J. Geophys. Res.*, **101**(D1), 2011–2023.

Arimoto, R., and coauthors, 1997: Comparison of trace constituents from ground stations and the DC-8 aircraft during PEM-WEST B. *J. Geophys. Res.*, **102**, 28539–28550.

Chan, L. Y., H. Y. Liu, K. S. Lam, and T. Wang, 1996: Observations of total column O_3 and vertical O_3 distribution at subtropical Hong Kong. Proceedings of the XVIII Quadrennial Ozone Symposium, L'Aquila, Italy, 12–21 September, 107–110.

Chan, L.Y., H. Y. Liu, and K. S. Lam, 1998a: Analysis of the seasonal behavior of tropospheric ozone at Hong Kong. *Atmos. Environ.*, **32(2)**, 159–168.

Chan, L. Y., C. Y. Chan, and Y. Qin, 1998b: Surface ozone pattern in Hong Kong. *J. Appl. Meteor.*, **37**(10), 1153–1165.

Derwent, R. G., P. G. Simmonds, and W. J. Collins, 1994: O_3 and CO measurements at a remote maritime location, Mace Head, Ireland, from 1990 to 1992. *Atmos. Environ.*, **28**(16), 2623–2637.

Draxler, R. R., and G. D. Hess, 1997: Description of the Hysplit_4 modeling system. *NOAA Technical Memorandum*, ERL ARL-224, Silver Springs, MD, December 1997.

Draxler, R. R., and G. D. Hess, 1998: An overview of the Hysplit_4 modeling system for trajectories, dispersion and deposition. *Aust. Meteor. Mag.*, **47**, 295–308.

Harris, J. M., and J. D. Kahl, 1990: A descriptive atmospheric transport climatology for the Mauna Loa Observatory using clustered trajectories. *J. Geophys. Res.*, **95**(D9), 13651–13667.

Harris, J. M., P. P. Tans, E. J. Dlugokencky, K. A. Masarie, P. M. Lang, S. Whittlestone, and L. P. Steele, 1992: Variations in atmospheric methane at Mauna Loa Observatory related to long-range transport. *J. Geophys. Res.*, **97**, 6003–6010.

Kato, N., and H. Akimoto, 1992: Anthropogenic emissions of SO_2 and NO_x in Asia: Emission inventories. *Atmos. Environ.* **26**(A), 2997–3017.

Khalil, M. A. K., and R. A. Rasmussen, 1988: Carbon monoxide in the Earth's atmosphere: Indications of a global increase. *Nature,* **332**, 242–245.

Lam, K. S., T. J. Wang, L. Y. Chan, and H. Y. Liu, 1996: Observation of surface ozone and carbon monoxide at a coastal site in Hong Kong. Proceedings of the XVIII

Quadrennial Ozone Symposium, L'Aquila, Italy, 12–21 September, 395–398.

Lam, K. S., T. J. Wang, L. Y. Chan, T. Wang, and J. M. Harris, 2001: Flow patterns influencing the seasonal behavior of surface ozone and carbon monoxide at a coastal site near Hong Kong. *Atmos. Environ.* **35(18)**, 3121–3135.

Liu, H. Y., W. L. Chang, and S. J. Oltmans, 1999: On springtime high ozone events in the lower troposphere from Southeast Asian biomass burning. *Atmos. Environ.* **33**(11), 2403–2410.

Liu, C. M., H. W. Chang, and S. C. Liu, 1999: An analysis of Lanyu baseline measurement data. *Atmos. Sci.*, **27**(2), 99–129. (in Chinese)

Parrish, D. D., J. S. Holloway, M. Trainer, P. C. Murphy, G. L. Forbes, and F. C. Fehsenfeld, 1993: Export of North American ozone pollution to the North Atlantic Ocean. *Science,* **259**, 1436–1439.

Parrish, D. D., M. Trainer, J. S. Holloway, J. E. Yee, M. S. Warshawsky, and F. C. Fehsenfeld, 1998: Relationships between ozone and carbon monoxide at surface sites in the North Atlantic Ocean. *J. Geophys. Res.*, **103**(D11), 13357–13376.

Pochanart, P., J. Hirokawa, Y. Kajii, and H. Akimoto, 1999: Influence of regional-scale anthropogenic activity in northeast Asia on seasonal variations of surface ozone and carbon monoxide observed at Oki, Japan. *J. Geophys. Res.*, **104**(D3), 3621–3631.

Streets, D. G., and S. T. Waldhoff, 2000: Present and future emissions of air pollutants in China: SO_2, NOx, and CO. *Atmos. Environ.*, **34**, 363–374.

Stunder, B. J. B., 1996: An assessment of the quality of forecast trajectories. *J. Appl. Meteor.*, **35**(8), 1319–1331.

Wayne, R. P., 1991: *Chemistry of Atmospheres*: *An Introduction to the Chemistry of the Atmospheres of Earth, the Planets, and Their Satellites*. Oxford University Press, 581pp.

Wang T., K. S. Lam, and Chan L. Y., 1997: Trace gas measurements in coastal Hong Kong during the PEM-WEST B. *J. Geophys. Res.*, **102**(D23), 28575–28588.

Wang T., K. S. Lam, A. S. Y. Lee, Pang S. W., and W. S. Tsui, 1998: Meteorological and chemical characteristics of the photochemical ozone episodes observed at Cape D'Aguilar in Hong Kong. *J. Appl. Meteor.*, **37**, 1167–1177.